Design Issues for the Active Control System of the California Extremely Large Telescope (CELT)

Gary Chanan[a], Jerry Nelson[b], Catherine Ohara[a], and Edwin Sirko[a]

[a] University of California, Irvine, Department of Physics and Astronomy, Irvine, CA 92697
[b] University of California, Santa Cruz, Department of Astronomy and Astrophysics
Santa Cruz, CA 95064

ABSTRACT

We explore issues in the control and alignment of the primary mirror of the proposed 30 meter California Extremely Large Telescope and other very large telescopes with segmented primaries (consisting of 1000 or more segments). We show that as the number of segments increases, the noise in the telescope active control system (ACS) increases, roughly as $\sqrt{n}$. This likely means that, for a thousand segment telescope like CELT, Keck-style capacitive sensors will not be able to adequately monitor the lowest spatial frequency degrees of freedom of the primary mirror, and will therefore have to be supplemented by a Shack-Hartmann-type wavefront sensor. However, in the case of segment phasing, which is governed by a "control matrix" similar to that of the ACS, the corresponding noise is virtually independent of n. It follows that reasonably straightforward extensions of current techniques should be adequate to phase the extremely large telescopes of the future.

Keywords: segmented mirrors, telescopes, phasing

1. INTRODUCTION

In the design of large segmented mirror telescopes, such as the ten meter Keck telescopes[1], the proposed 30 m California Extremely Large Telescope (CELT)[2], and the proposed 100 m OWL telescope[3], a key issue is to determine the optimal number of segments (for a given telescope diameter). Several factors favor many smaller segments. Since the required segment thickness varies as the square of the segment diameter, smaller segments can mean a significantly smaller moving mass of the telescope and a significantly smaller cost for the mirror material. Smaller segments are also much easier to fabricate by means of stressed mirror polishing or ion beam figuring techniques. However, other factors favor fewer, larger segments. Specifically, (because there are more of them) smaller segments are more difficult to control (via an active control system) and are more difficult to align – and in particular – to phase.

The two Keck telescopes each consist of 36 hexagonal segments, 0.9 m on a side (1.8 m circumscribed diameter). Since issues of cost and weight are of paramount importance for extremely large telescopes, and since our experience at Keck has been that segment figure issues have been more problematic than issues of alignment and control, we are led to consider smaller segments for the design of CELT. Figure 1 shows the current baseline design of CELT, with 1098 hexagonal segments each 0.5 m on a side, covering its nominally 30 m aperture; the Keck primary mirror is shown alongside to scale. In this paper, we explore quantitatively the implications of this large number of segments for telescope alignment and control, and show that the resulting complications are modest and straightforward to deal with.

2. ACTIVE SEGMENT CONTROL

In this Section, we first briefly review the Keck Active Control System. We then outline a scheme for classifying the misalignments of the Keck and similar segmented telescopes in terms of the modes of the primary mirror. Finally, we utilize this modal analysis to provide some quantitative insight into the active control systems for CELT and other extremely large segmented telescopes of the future.
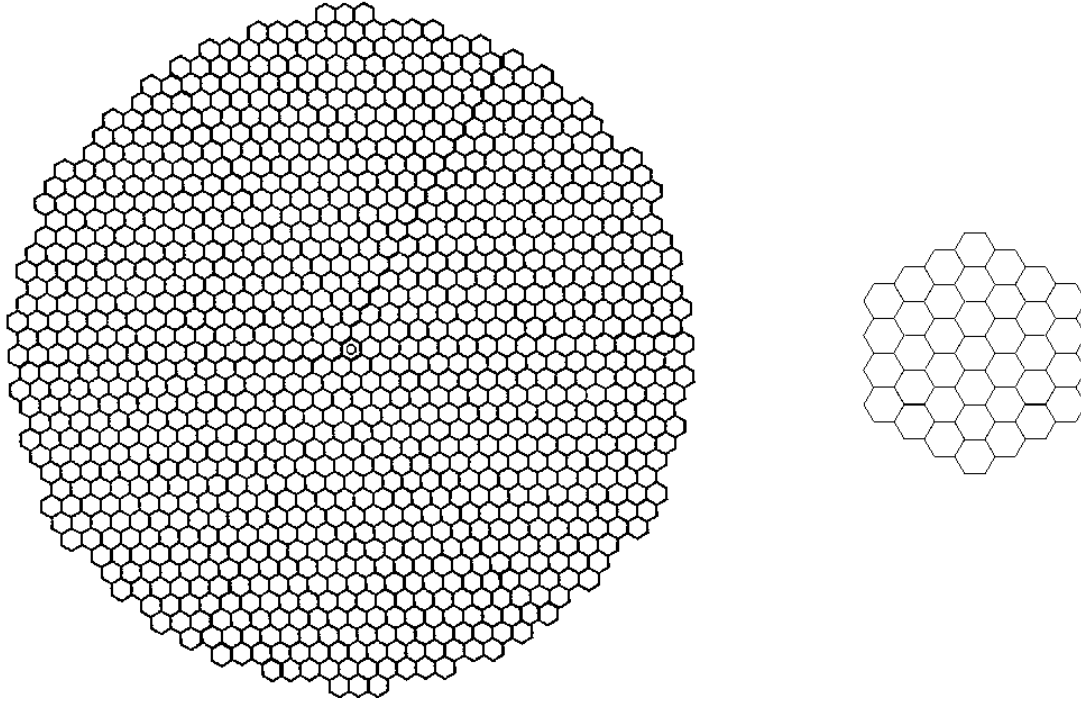
Figure 1. Geometry of the proposed CELT primary mirror. The Keck mirror geometry is shown to scale for comparison.

2.1 REVIEW OF KECK ACS

The Keck Active Control System (ACS) consists of 108 mechanical actuators (three for each segment, to control the out-of-plane degrees of freedom) and 168 capacitive displacement sensors (two along each intersegment edge).[2] Once the desired sensor readings are determined (by independent optical means[4]), the actuators are updated at 2 Hz in order to continually drive the actual sensor readings to their desired values. [Three "virtual sensors" constrain the primary mirror in piston, tip, and tilt, since the ACS does not sense these global rigid body degrees of freedom.] In this way the primary mirror is frozen or stabilized against changes caused by gravity, wind, and temperature drifts.

Of course, the sensors are not perfect, and any (electronic) noise fluctuations in the sensors will cause the actuators to move. Thus, the active control system contributes to the overall wavefront error of the telescope. [Since the RMS actuator fluctuation is about equal to the RMS surface fluctuation, the corresponding wavefront error is about equal to twice the RMS actuator fluctuation.] For Keck, the optical error budget allots 58 nm for this contribution to the wavefront error.[5]

2.2 NORMAL MODES OF THE PRIMARY MIRROR

To gain some insight into the noise propagation from sensors to actuators and hence to wavefront error, it is convenient to describe an arbitrary configuration of the Keck – or any similarly controlled – primary in terms of the "normal modes" of the mirror.[6] Here we use the phrase not in the context of vibrational normal modes, but rather of the eigenvectors associated with the singular value decomposition of the control matrix of the active control system. We describe these briefly in the following.

Changes in the lengths of the actuators (three per segment) which control the primary produce corresponding changes in the readings of the edge sensors (two per intersegment edge). The relationship is linear:

$$s_i = \sum A_{ij}\, a_j$$

where the s_i are the changes in the sensor readings, a_j are the changes in the actuator lengths, and A_{ij} is the control matrix for the system. The matrix A_{ij} is determined by the sensor and actuator geometry. The desired sensor readings are defined when the telescope is properly aligned optically; the actuator lengths are changed further only to maintain these desired sensor readings in the face of deformations due to gravity, temperature changes, and so on. The appropriate actuator changes which will maintain the null sensor readings are calculated with the aid of the pseudo-inverse matrix B_{ji}:

$$a_j = \sum B_{ji}\, s_i$$

The B-matrix is constructed by singular value decomposition of the original matrix.[7] In the course of this process, one constructs an essentially unique basis set of actuator vectors, a_k. We refer to the vectors in this basis set as the normal modes of the system. The component a_{ik} specifies the length of the ith actuator in the kth normal mode. As is typical in problems of this sort, some of the modes are singular – in this case, the three actuator vectors corresponding to rigid body motion of the primary mirror as a whole (since such motion has no effect on the sensor readings). Therefore, if there are n segments, there are $3n$ actuators, and $3n-3$ modes of interest in the basis set. These vectors are normalized in the sense:

$$\sum_i a_{ik}^2 = 3\,n$$

That is, the right-hand side of Eq. (3) is the total number of actuators, not the total number of modes.

If we were to put random noise into the sensors, then the actuators would respond proportionally in a way that is completely defined by the matrix A_{ij}:

$$\delta a = \alpha\, \delta s$$

where δs and δa are the RMS values of the sensors and actuators, and we refer to the factor α as the (overall) noise multiplier. Alternatively, we could put random noise into the sensors and determine the RMS amplitude $\delta\alpha_k$ of each of the above $3n-3$ modes. In this way we can associate an individual noise multiplier $\delta\alpha_k$ with each mode:

$$\delta a_k = \alpha_k\, \delta s$$

The modes are orthonormal in the sense[7]:

$$\delta a^2 = \sum \delta a_k^2 = \sum \alpha_k^2\, \delta s^2$$

It is convenient to order the modes according to the size of their error multipliers, from largest to smallest. With this ordering it is useful to define a residual error multiplier r_k, which includes the error multiplier of the kth mode and all higher modes:

$$r_k^2 = \sum_k^{3n-3} \alpha_j^2$$

[Note that r_1 is then the same as the global error multiplier α.] When the modes are ordered in this way, they are also more or less ordered in spatial frequency from lowest to highest. The reason for this correspondence is not hard to understand: low spatial frequency modes have small edge discontinuities which are difficult for the sensors to detect and therefore for the ACS to control; high spatial frequency modes have large edge discontinuities which are easily detected by the edge sensors.

Figure 2 presents surface plots of primary mirror modes of the Keck telescope, illustrating the general trend that spatial frequency (and degree of edge discontinuity) increases with increasing mode number. In particular, mode 1, which has the highest noise multiplier, or equivalently is controlled the most poorly, has the lowest spatial frequency – it corresponds to the actuators lying on the surface of a paraboloid. This mode is known as "focus mode" since it resembles a faceted version of

the error surface of a defocused monolithic telescope. By contrast, mode 105 has a high spatial frequency and highly discontinuous edges, which are easily detected by the sensors and thus well-controlled by the ACS.

For the Keck geometry, the overall noise multiplier[6] is $\alpha = 4.42$. Although under laboratory conditions the RMS sensor electronic noise is less than 1 nm, in the telescope it is about 6 nm. Thus, the ACS contribution to the wavefront error is 53 nm, which is within the error budget. We believe it is likely, however, that in future implementations the sensor electronic noise can be reduced by a factor of several.
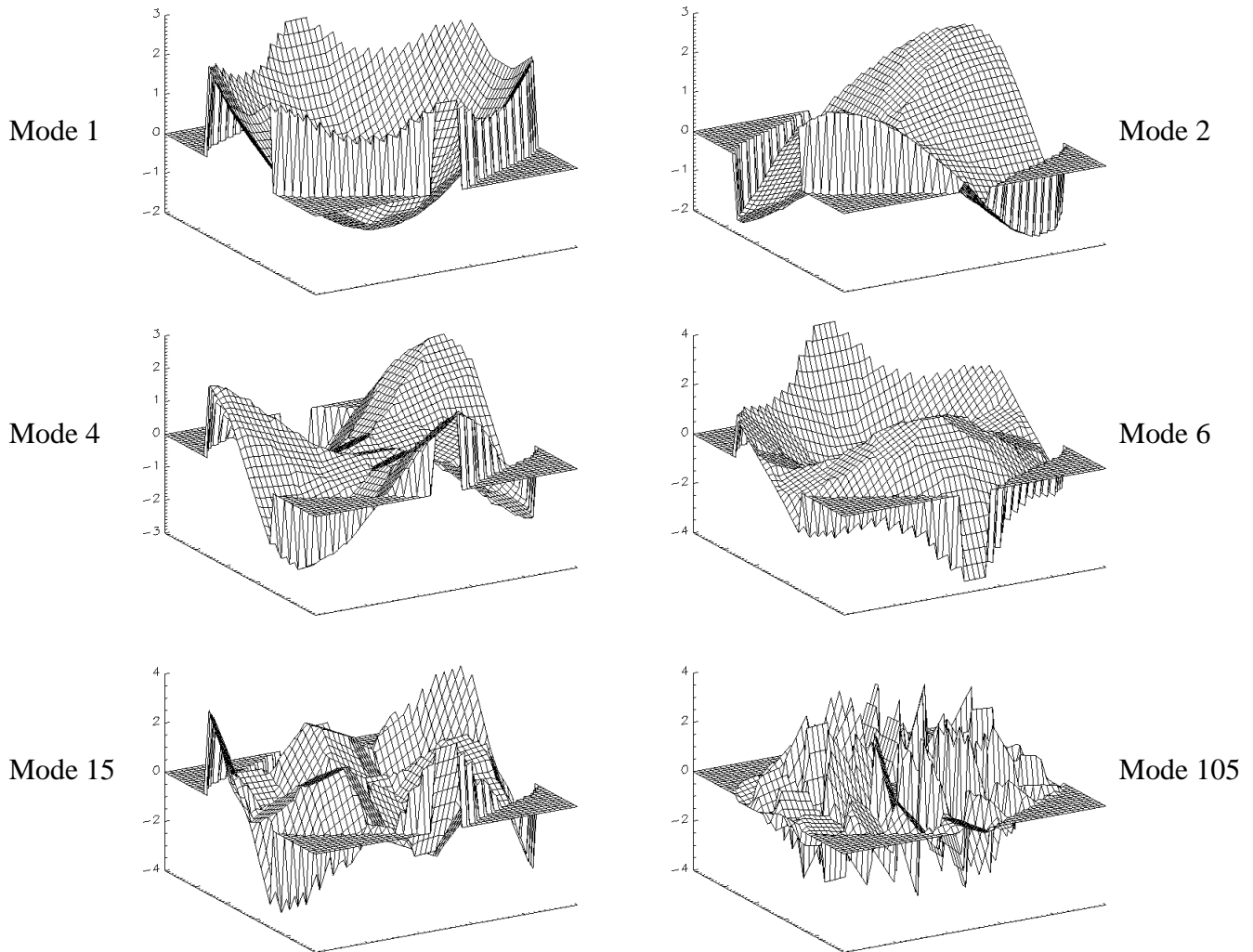
Figure 2. Surface plots of several Keck primary mirror modes, illustrating the general trend that spatial frequency and edge discontinuity increase with mode number.

2.3 CELT ACS

In order to infer the scaling properties of the active control system, we consider not only the 1098 segment CELT telescope, but also several possible designs intermediate between Keck and CELT. Keck consists of three hexagonal rings; we also consider telescopes of five, seven, and eleven hexagonal rings. [These are not shown explicitly but can be seen within the CELT outline of Figure 1.] The numbers of segments, actuators, and sensors of these telescopes are shown in Table 1. Note that although the outermost segments of CELT would belong to the twenty-first ring, the CELT primary mirror is circularized (to minimize the overall diameter and diffraction effects), so the last few hexagonal rings are not complete.

We can construct the control matrices for all of these telescopes by assuming the same relative positioning of actuators and sensors on each segment as for Keck. The noise multipliers with which we are concerned are independent of the size of the segments (if the number and arrangement of the segments are fixed). The individual mode error multipliers for Keck, the 7-ring telescope, and CELT are shown as a function of mode number in Figure 3. For the low order modes, these multipliers scale with the number of segments roughly as $\sqrt{n}$. Since these low order multipliers dominate the global multiplier α, this also grows as $\sqrt{n}$. Whereas α was 4.42 for Keck, it is 21.60 for CELT (see Table 1).

The optical error budget for CELT is currently more challenging than for Keck; only 30 nm is allotted to the ACS contribution to the wavefront error. Clearly, then, the growth of the global noise multiplier with the number of segments is a concern. For the nominal 6 nm sensor noise, the wavefront error would be 259 nm or an alarming 8.6 times the error budget allocation.

However, because the noise multiplier is a rapidly decreasing function of mode number, this problem can be addressed in a straightforward manner, in particular by sensing only a few tens of the lowest order modes by separate means. In Figure 4 we plot the residual noise multiplier for the various telescopes in Table 1. By inspection of the figure, it is clear that we can obtain the desired eight-fold reduction in the ACS-induced wavefront error if the first 50 modes are sensed, say, by a Shack-Hartmann wavefront sensor. For adaptive optics applications, such a sensor would already be an integral part of the AO system. For non-AO applications, where the optical quality demands on the telescope are much reduced, a low bandwidth Shack-Hartmann sensor handling the lowest few modes would probably suffice. If we can effect an expected factor of 2 or 3 reduction in sensor noise, the demands on the wavefront sensor would be more modest still. Note that in any case the ACS would still be required to sense the more than 3200 remaining higher order distortions of the primary mirror, and (by Figure 4), it should do an excellent job of this.

As long as we are forced to this two-tiered approach to segment position sensing, we can simplify the sensors substantially. At Keck the sensors interlock underneath the segments. Sensors of this complicated geometry are expensive to build and they make segment exchanges difficult. However, consider instead capacitive sensors that are located directly on the segment edges, as shown schematically in Figure 5. Such sensors are vastly simpler mechanically, and segment exchanges would be greatly facilitated, since the sensors would not need to be rotated out of the way to remove or install a segment. The problem with this sensor geometry is that these "zero-offset" sensors are blind to mode 1 or focus mode, which becomes singular when the sensor offsets go to zero. However, since we have shown above that it will be necessary on other grounds to sense low order modes by some external means, this additional singular mode does not represent a problem. Figure 6 shows that (except for focus mode) the residual noise multiplier for this zero offset sensor geometry is not much different than for the Keck sensor geometry.

**Table 1.** Parameters of Various Segmented Telescopes

| Telescope	Segments	Actuators	Sensors	ACS Noise Multiplier	Phasing Noise Multiplier
Keck	36	108	168	4.42	0.620
5-ring	90	270	468	6.57	0.640
7-ring	168	504	912	8.78	0.657
11-ring	396	1188	2232	13.27	0.683
CELT	1098	3294	6336	21.60	0.714
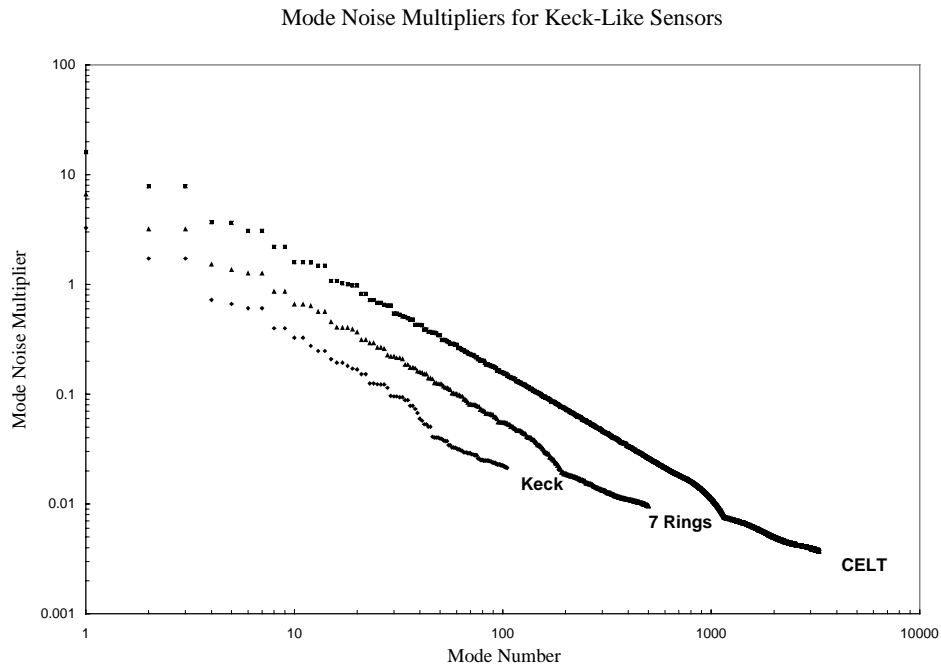
Figure 3. Mode noise multipliers for three of the segmented telescope designs in Table 1. The low order noise multipliers increase approximately as the square root of the number of segments. Placement of actuators and sensors on a segment is assumed identical to that of the Keck telescope in all cases.
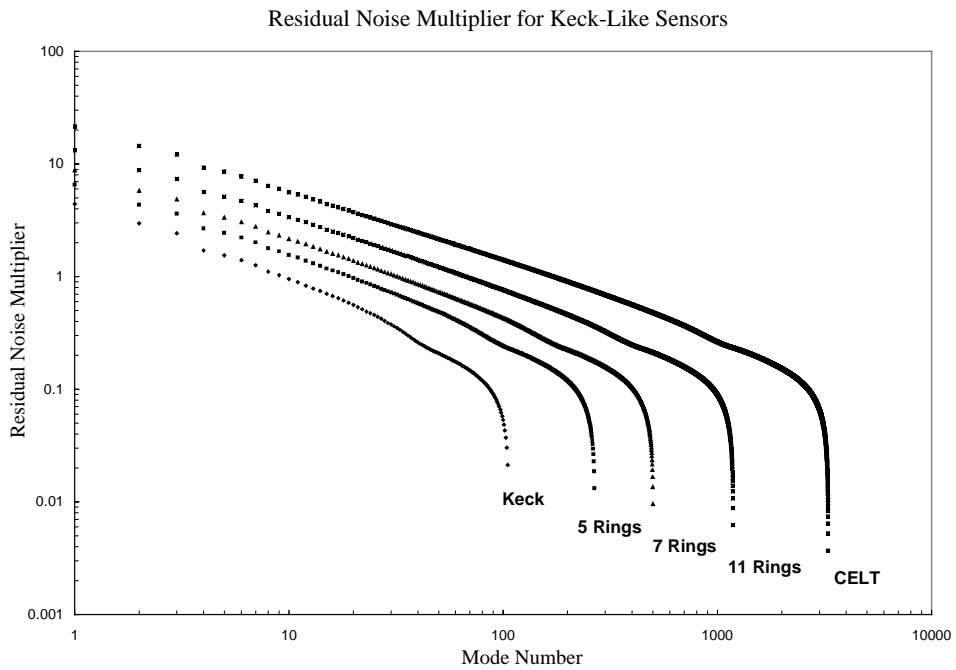
Figure 4. Same as Figure 3, but showing residual noise multipliers (as defined in text), not individual noise multipliers, for all five of the segmented telescope designs in Table 1.
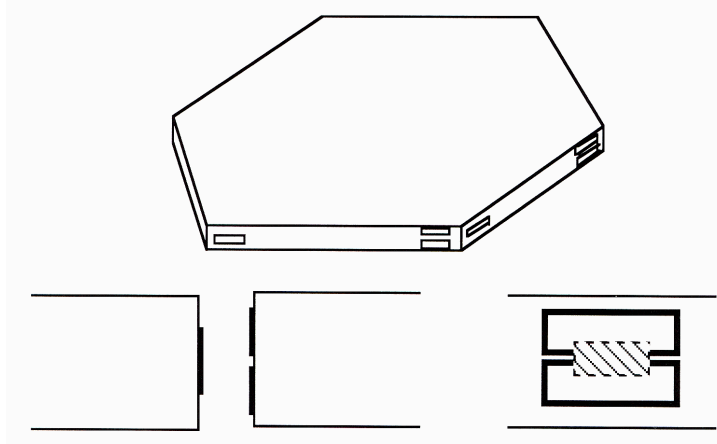
Figure 5. Conceptual drawing of proposed non-interlocking CELT edge sensor. Such sensors are blind to focus mode distortions of the primary.

Residual Noise Multipliers for Zero-Offset Sensors
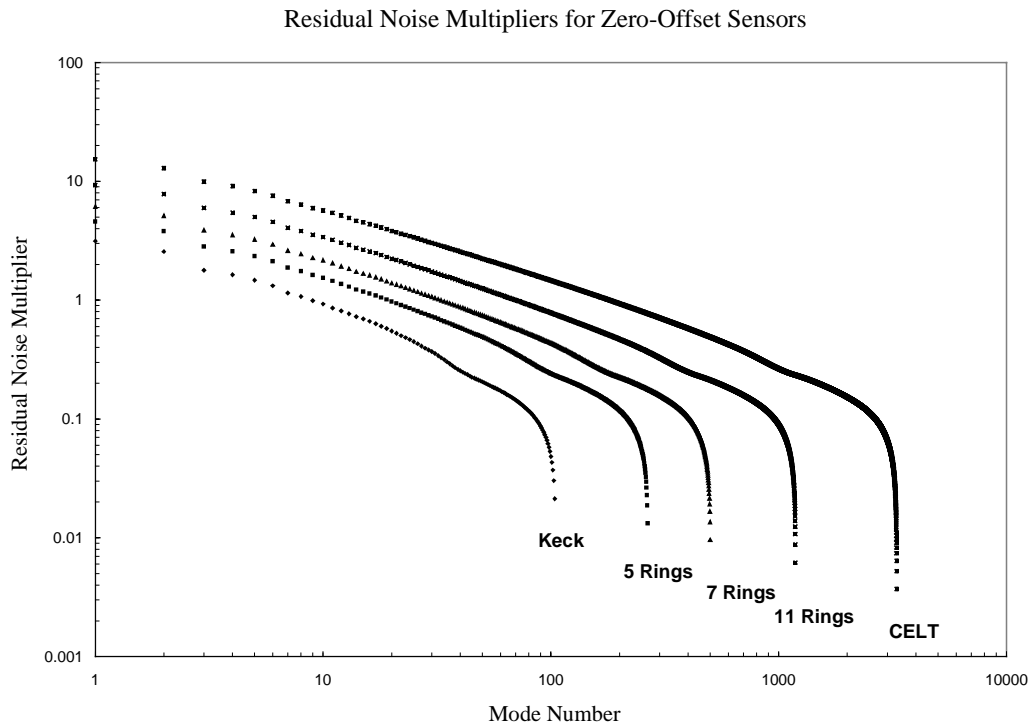
Figure 6. Same as Figure 4, but for the non-interlocking sensor geometry of Figure 5, rather than the Keck sensor geometry assumed in Figure 4.

3. PHASING

The active control systems under consideration here are electro-mechanical in nature. It is still necessary to provide (periodically) an optical reference to align the telescope properly. At Keck it has proved convenient to break the segment alignment problem up into two parts: segment tip/tilt and segment piston. The former can be accomplished in a straightforward way by geometrical optics techniques; here we concentrate on the more difficult latter problem, also known as segment phasing.

3.1 REVIEW OF KECK PHASING

We currently phase the segments of the Keck telescopes by two different techniques – a Shack-Hartmann technique[8,9] which results in piston errors below 10 nm (wavefront errors below 20 nm), and an extra-focal technique which results in piston errors of 40 nm (80 nm wavefront).[10] The former technique is more than adequate to meet the Keck optical error budget term for phasing of 50 nm (wavefront)[4], or even, for that matter, the more stringent CELT goal of 25 nm (wavefront). However, the latter technique (whose ultimate sensitivity has probably not been reached), will require some improvement if it is to be useful for this purpose.

3.2 CELT PHASING

Although the physical size of the instrumentation required for Shack-Hartmann phasing grows with the size of the telescope, and the sizes of the required lenslet array and charge coupled device grow with the number of segments, these requirements are probably not prohibitive for extremely large telescopes such as CELT or even OWL. We have shown[11] that a 2k x 2k CCD should be adequate for this purpose for CELT and a 4k x 4k CCD should be adequate for OWL.

One concern for phasing large telescopes is error propagation. The Shack-Hartmann measurements determine intersegment edge heights; these are converted to piston errors by a linear system of equations related to those which govern the telescope ACS. Since there are half as many edges as sensors, the "control matrix" for CELT phasing is 1098 x 3168, compared to the 3294 x 6336 ACS matrix. However, while the ACS noise multiplier grows like $\sqrt{n}$, so that the CELT multiplier is nearly 5 times that of Keck, the corresponding phasing noise multiplier is almost independent of n (See Table 1) – the CELT multiplier is only 15% larger than is Keck's. It follows that the accuracy of Shack-Hartmann phasing should not decrease as the number of segments increases, and the tools for phasing extremely large telescopes should require only modest extrapolation of existing tools.

As an example of the potential application of a current Keck phasing technique to CELT we consider the extra-focal curvature sensing type scheme known as Phase Discontinuity Sensing.[10] In its current implementation at Keck, PDS has a capture range of +/- 400 nm and an accuracy of 40 nm, as noted above. Therefore consider a Monte Carlo simulation in which a CELT primary mirror has its 1098 random segment piston errors initially drawn from a flat distribution between +400 nm and - 400 nm (corresponding to an RMS piston error of 233 nm). A representation of the primary mirror and the corresponding out-of-focus image is shown in Figure 7. Here the wavelength is 3.3 microns and the detector is 130 arcseconds on a side. After 12 iterations of the PDS algorithm, the RMS piston error was reduced to 22 nm (Figure 8) – a substantial improvement. We are continuing to develop this technique both at Keck and via simulations, in order to extend the capture range, improve the accuracy, and increase the rate of convergence. The PDS approach is particularly attractive for extremely large telescopes such as CELT because no specialized instrumentation is required; virtually any infrared science camera should suffice.
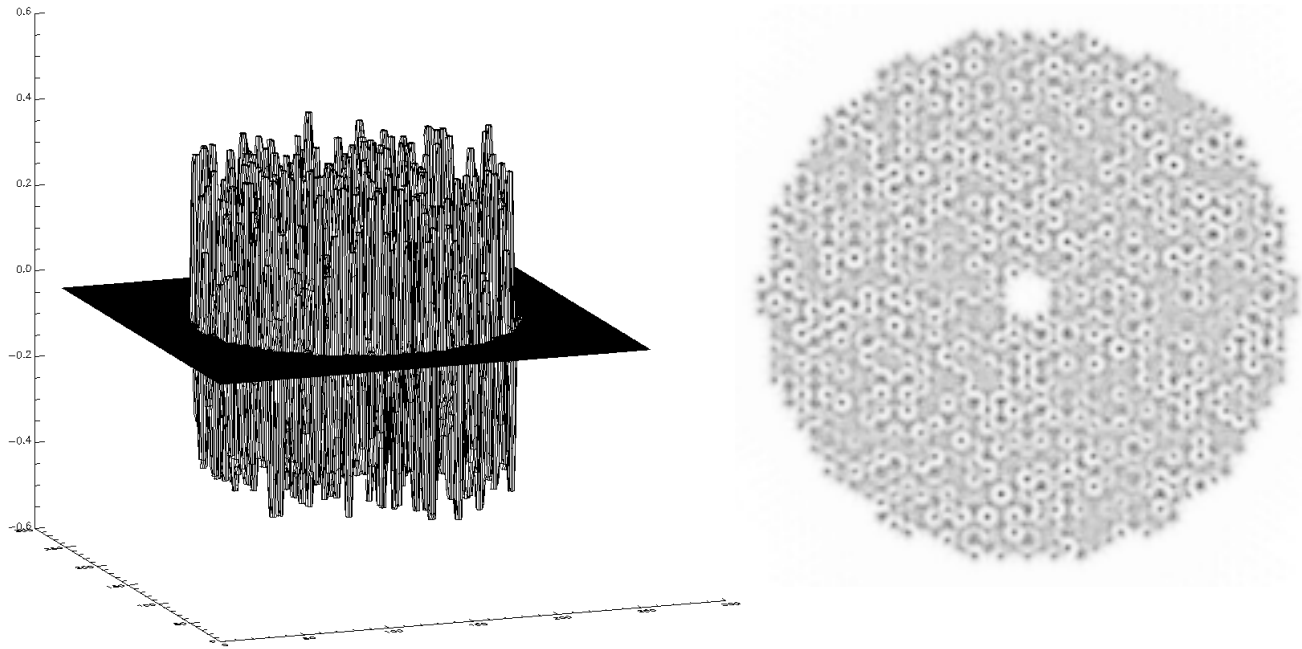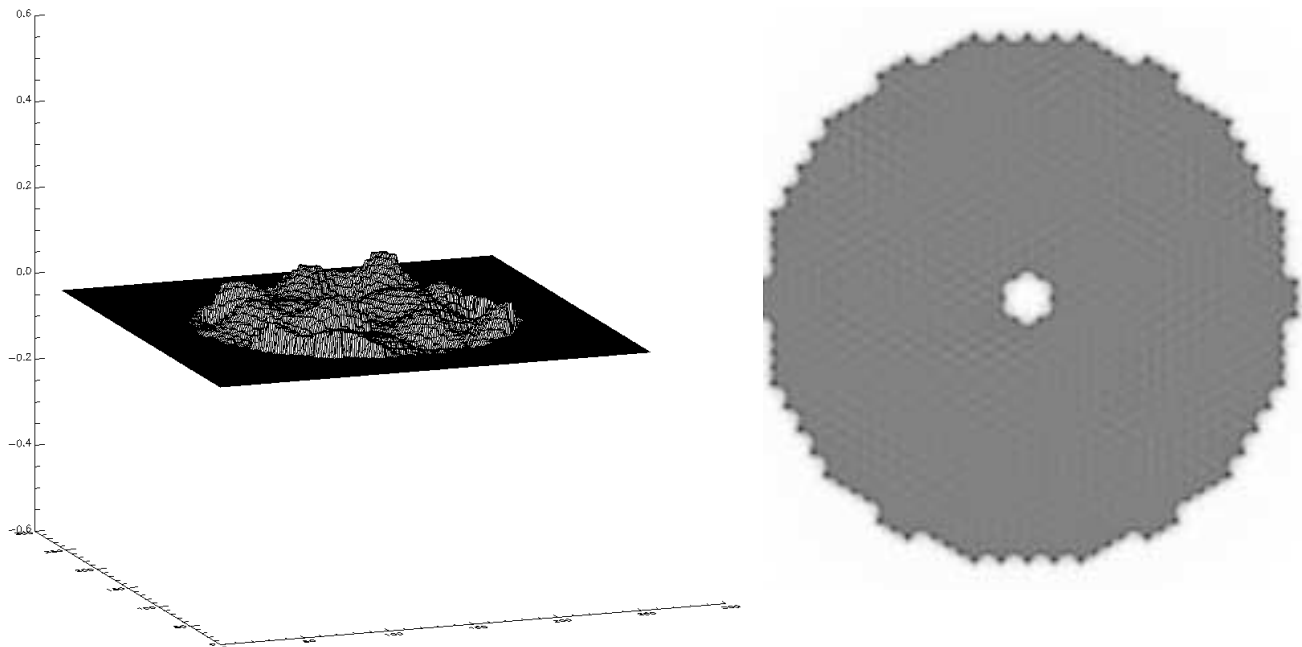
Figure 7. CELT primary mirror at the start of a PDS phasing simulation together with the corre sponding out of focus image. The initial piston errors have an RMS of 233 nm.

Figure 8. Same as Figure 7, but after 12 iterations of the PDS algorithm. The final RMS piston error is 22 nm.

REFERENCES

1. J. E. Nelson, T. S. Mast, and S. M. Faber, "The design of the Keck Observatory and telescope," Keck Observatory Report 90 (W. M. Keck Library, Kamuela Hawaii, 1985), pp. 5-1 to 5-44.
2. J. E. Nelson and T. Mast, "Giant optical devices," in *Proceedings of the Backaskog Workshop of Extremely Large Telescopes,* T. Anderson, ed., pp. 1-11, Lund University and ESO, June 1999.
3. R. Gilmozzi, B. Delabre, P. Dierickx, N. Hubin, F. Koch, G. Monnet, M. Quattri, F. Rigaut, R. N. Wilson, "The Future of Filled Aperture Telescopes: is a 100m Feasible?," in *Advanced Technology Optical/IR Telescopes VI*, L. M. Stepp, ed., vol. 3352, pp. 778-791, SPIE, 1998.
4. G. Chanan, J. Nelson, T. Mast, P. Wizinowich, and B. Schaefer, "The W. M. Keck telescope phasing camera system," in *Instrumentation in Astronomy VIII,* D. L. Crawford and E. R. Craine, eds., vol. 2198, pp. 1139-1150, SPIE, 1994.
5. G. Chanan, G. Djorgovski, A. Gleckler, S. Kulkarni, T. Mast, C. Max, J. Nelson and P. Wizinowich, eds., "Adaptive optics for Keck Observatory," Keck Observatory Report 208 (W. M. Keck Library, Kamuela Hawaii, 1996), pp. 3-26 to 3-36.
6. M. Troy, G. A. Chanan, E. Sirko, and E. Leffert, "Residual misalignments of the Keck telescope primary mirror segments: classification of modes and implications for adaptive optics," in *Advanced Technology Optical/IR Telescopes VI*, L. M. Stepp, ed., vol. 3352, pp. 307-317, SPIE, 1998.
7. W. Press, B. Flannery, S. Teukolsky, and W. Vetterling, *Numerical Recipes: the Art of Scientific Computing*, pp. 52-64, 502-515. Cambridge University Press, New York, 1989.
8. G. A. Chanan, M. Troy, F. G. Dekens, S. Michaels, J. Nelson, T. Mast, and D. Kirkman, "Phasing the mirror segments of the Keck telescopes: the broadband phasing algorithm," *Applied Optics* **37**, pp. 140-155, Jan. 1998.
9. G. A. Chanan, C. Ohara, and M. Troy, "Phasing the mirror segments of the Keck telescopes II: The Narrowband Phasing Algorithm," (preprint).
10. G. A. Chanan, M. Troy, and E. Sirko, "Phase discontinuity sensing: A method for phasing segmented mirrors in the infrared," *Applied Optics* **38**, pp. 704-713, Feb. 1999.
11. G. A. Chanan, M. Troy, and C. Ohara, "Phasing the primary mirror segments of the Keck telescopes: A comparison of different techniques," *in Optical Design, Materials, Fabrication, and Maintenance*, P. Dierickx, ed., vol. 4003, SPIE, 2000.